GyFoam: Fabricating Lattice Foam with Customizable Stiffness through Uniform Expansion

Guanyun Wang
Zhejiang University
Hangzhou, China
guanyun@zju.edu.cn

Haotian Chen
Zhejiang University
Hangzhou, China
haotian_chen@zju.edu.cn

Yufeng Wang
Zhejiang University
Hangzhou, China
wyufeng@zju.edu.cn

Songyun Li
Zhejiang University
Hangzhou, China
3210100157@zju.edu.cn

Yue Tao
Zhejiang University
Hangzhou, China
1200410029@zust.edu.cn

Fanke Qi
Zhejiang University
Hangzhou, China
fankeqi@u.nus.edu

Lizhuo Cao
Zhejiang University
Hangzhou, China
3210101610@zju.edu.cn

Xiao Jin
Imperial College London
London, United Kingdom
xj521@ic.ac.uk

Ye Tao*
Hangzhou City University
Hangzhou, China
taoye@hzcu.edu.cn

Jiaji Li*
Massachusetts Institute of Technology
Cambridge, USA
jiaji@mit.edu

Figure 1: Examples of GyFoam applications: (a) Bunny sculpture before and after heating; (b) Mattress and pillow; (c) Midsole; (d) Kneepad; (e) Interactive lamp.

Abstract

We present GyFoam, a fabrication method integrating foam material with lattice structure to enable controlled and uniform expansion, which supports high-quality forming in appearance and customizable stiffness in function, using standard 3D printers, filaments, commercially available Thermo-Expandable Microspheres and silicone. To achieve customizable stiffness, we propose two methods: modifying material concentration and adjusting lattice structural parameters. Additionally, we propose three shape control strategies for creating complex shapes: bending, wavy edges, and internal doming. Furthermore, a user-friendly design tool is established for users to construct lattice structures, preview basic deformation, and generate mold models for printing. Finally, through a series of applications, we validate GyFoam's practical usage of fabricating large objects, wearable products, enabling flexible interactions and creating aesthetic designs.

CCS Concepts

• **Human-centered computing → Human computer interaction (HCI)**.

Keywords

Fabrication, Foam material, Uniform Expansion, Customizable stiffness

ACM Reference Format:
Guanyun Wang, Haotian Chen, Yufeng Wang, Songyun Li, Yue Tao, Fanke Qi, Lizhuo Cao, Xiao Jin, Ye Tao, and Jiaji Li. 2025. GyFoam: Fabricating Lattice Foam with Customizable Stiffness through Uniform Expansion. In *The 38th Annual ACM Symposium on User Interface Software and Technology*

*Corresponding authors

UIST '25, Busan, Republic of Korea

ACM ISBN 979-8-4007-2037-6/25/09
https://doi.org/10.1145/3746059.3747785

(UIST '25), September 28–October 01, 2025, Busan, Republic of Korea. ACM, New York, NY, USA, 16 pages. https://doi.org/10.1145/3746059.3747785

1 INTRODUCTION

With the development and widespread adoption of personal fabrication, human-computer interaction (HCI) research is increasingly focused on exploring soft materials [29, 46, 52, 60] and programmable structures [21, 28, 54] to create safer and more adaptive physical interfaces. To further facilitate the fabrication for complex shapes and adjustable mechanical properties, researchers have explored a range of mechanisms, including inflatable structures [37, 38, 61, 68], metamaterials [20, 28, 51], and hybrid fabrication approaches [30, 61]. In general, creating interactive objects with controllable shapes and mechanical properties is increasingly becoming a prominent trend in HCI.

Foaming technologies enable the fabrication of lightweight, expandable materials that feature micro-porous structures and superior energy absorption performance [22, 66]. Among these techniques, physical foaming with Thermo-Expandable Microspheres (TEMs) has gained widespread attention because of its simple process and cost-effectiveness.This approach allows composites containing TEMs to undergo significant volumetric expansion upon high-temperature activation while maintaining desirable elasticity. These characteristics have attracted increasing research interest. For example, Cai et al. [5] investigated the energy absorption capabilities of composites made from TEM and PDMS; Yang et al. [69] utilized TEMs to construct microstructures for highly sensitive flexible pressure sensors, targeting wearable devices and health monitoring applications. Within HCI community, Kaimoto et al. [23] combined TEMs with UV-curable elastic adhesives to produce expandable solid objects. However, these studies primarily focused on simple geometries, leaving significant opportunities for leveraging TEMs to fabricate complex three-dimensional shapes and tunable mechanical stiffness.

While TEMs can achieve substantial volumetric expansion, fabricating geometrically complex objects remains inherently challenging. First, their inherent thermal insulation properties [7] lead to uneven heating within solid objects, particularly for larger volumes, causing overheating of the outer layers while leaving the inner regions insufficiently heated. This results in non-uniform and incomplete expansion [23]. Second, expansion creates micro-porous structures that provide additional flexibility, which intrinsically couples the material's stiffness with its degree of expansion [5]. This coupling makes it difficult to adjust stiffness independently. To address these issues, we introduce lattice structures. Due to their controllable porosity [18], lattice structures promote more uniform heat distribution and volumetric expansion, while also enabling independent control over the material's stiffness properties [33].

Therefore, we present GyFoam, a fabrication method integrating foam material with lattice structure to enable controlled and uniform expansion, which supports high-quality forming in appearance and customizable stiffness in function. GyFoam method allows general users to use common FDM 3D printers, standard filaments, commercially available TEM and silicone to easily fabricate lightweight and lattice-structured objects with customizable stiffness. To facilitate greater design personalization, we propose two stiffness tuning approaches—adjusting material concentration and lattice structural parameters—and three deformation control strategies—bending, wavy edges and internal doming. Additionally, we provide a user-friendly design tool to help novices quickly construct models, preview basic deformation effects, and generate printable mold files according to their needs. Finally, we demonstrate several practical application scenarios of GyFoam, including large objects, wearable products and soft tangible interfaces.

This paper presents the following contributions:

- A fabrication method combining foam material with lattice structure to achieve controlled and uniform expansion (up to 20-fold in volume) which enables high-quality foaming-driven shaping and customizable stiffness, using off-the-shelf materials and common equipment.
- Strategies to control stiffness and shape deformations using this new foaming method. Through experiments, we propose a predictive model to estimate the stiffness of the foamed material based on the concentration and lattice structural parameters. Additionally, we introduce three strategies for achieving controlled shape deformation.
- A tailored design tool to generate lattice-structured mold models. We develop software to enable users to preview lattice structures, visualize basic deformations, and generate printable mold files for 3D printing.
- Example applications. We explore the potential of our new foam materials in prototyping, personalized product fabrication and soft interfaces.

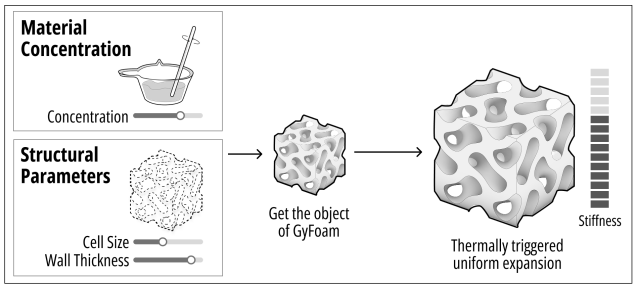

Figure 2: Using GyFoam method to make uniformly expandable objects with customizable stiffness.

2 RELATED WORK

2.1 Personal Fabrication of Expandable Objects with Controllable Shapes and Stiffness

The rapid advancement of personal fabrication technologies has provided users with a diverse range of tools and methods for rapid prototyping [35, 55, 56] and fabricating interactive devices [10, 59, 70]. However, fabricating objects with independent control over both shapes and mechanical properties remains a persistent challenge in personal fabrication.

Prior work has explored deformation-driven shaping, where forms emerge through material responses rather than direct fabrication. 4D printing enables self-bending [39, 44, 58] and self-folding behaviors [3]. Expansion-based shaping has also been introduced

using inflation, heat, or structural release. For example, PneuFab [61] combines 3D printing and blow molding for rapid shape formation, while Printflatables [50] and Pneumatic Laser Origami [43] support large-scale inflatable fabrication. Beyond shaping, tunable stiffness has been studied through strategies like truss structures [12, 53], metamaterials [20, 28, 51], and compliant mechanisms [16, 17, 34].

Some expandable systems further integrate stiffness control into the shaping process. Previous studies have explored methods for controlling the physical properties of inflatable structures. For example, PneuFab [61] controlled the stiffness by adjusting internal air pressure, after blowing the PLA model. Similarly, SnapInflatables [68] introduced a method for fabricating inflatable structures, allowing for tunable triggering forces and stiffness levels through structural design. Meanwhile, 3D printing with flexible materials like TPU has been used to create objects with customized shapes and stiffness [2, 19]. However, this method is constrained by printer size, and its stiffness tuning is typically limited to one direction—reducing stiffness relative to fully infilled structures through structural design or in-situ foaming.

Compared to the existing fabrication methods, GyFoam offers distinct advantages for fabricating expandable objects with high structural integrity due to the monolithic construction, free from structural discontinuities such as inflation ports or assembly seams.

2.2 Foam Materials as Tangible and Interactive Mediums

Foam materials are considered highly promising for constructing expandable objects. These materials achieve significant volumetric expansion by forming numerous cavities within their structure, resulting in advantageous properties such as lightweight, elasticity, and functional adaptability. Currently, foamed materials are commonly fabricated through mechanical foaming, chemical foaming, and physical foaming [22]. Researchers have explored the use of commercially available foamed materials to fabricate furniture-sized prototypes [27] and flexible sensors [40, 62]. Lazaro Vasquez et al. [31] explored the fabrication and application of bio-based foam materials, offering new aesthetic and functional possibilities for HCI.

Recently, foaming methods based on TEM have attracted researchers' attention due to their ease of fabrication and controllability. Researchers have combined TEMs with other substrate materials to enhance mechanical properties and achieve high energy absorption efficiency [5]. These efforts have also extended to applications such as constructing sensors [6, 7] and enabling detection for wearable devices [69]. Additionally, Liu et al. [36] proposed a 4D printing technique for foam materials with bilayer structures that transform from planar to three-dimensional shapes upon heating. In HCI, preliminary explorations have also been conducted. For example, ExpandFab [23] introduced a fabrication approach that combined TEMs with UV-curing elastic adhesive to produce expandable objects, demonstrating samples up to approximately 15 cm. While this approach effectively achieves significant expansion, some of the fully solid-filled structures presented in their work exhibited unevenness after expansion, due to the expanding TEMs which reduced the thermal conductivity. Moreover, the foaming-induced expansion directly determines the material's rigidity, which limits its customizability and tunability.

In our work, we further explore TEM as a physical foaming method, and integrate them with lattice structures to achieve controlled and uniform expansion. GyFoam enables high-quality, foaming-driven shape formation and tunable stiffness with improved consistency and design reliability.

2.3 Lattice Structures for Enhanced Interaction

Lattice structures are three-dimensional porous architectures composed of periodically arranged unit cells. Their lightweight nature, high specific surface area, and tunable mechanical properties have garnered significant attention in materials science and structural design [18, 33].

In recent years, HCI researchers have increasingly recognized the potential of lattice structures in personal fabrication and interaction design. Several studies have employed 3D printing technologies, such as FDM and SLA, to fabricate lattice structures with diverse physical properties and flexible deformation capabilities. These efforts have explored applications in sensing [32, 48], haptic feedback [49] and interactive interfaces [21, 47].

In GyFoam, we combine lattice structure with foam material to address the issue of uneven expansion. Moreover, lattice structures introduce new tunable factors, offering greater potential for mechanical performance modulation and unlocking broader design possibilities in both functionality and aesthetics.

2.4 Combining Foam Materials and Lattice Structures

Both researchers and commercial companies have recognized the tremendous potential of combining foam materials with lattice structures. For example, some studies [13, 63] have applied carbon dioxide physical foaming to 3D-printed lattice structures made from PLA and TPU, successfully fabricating lightweight structures with enhanced energy absorption efficiency. Moreover, Desktop Metal has introduced a foaming resin that can be printed through DLP technology and then expanded through heating. They demonstrated the application of this material by creating lattice-structured automotive cushions [9].

However, these existing approaches often rely on expensive industrial equipment or complex laboratory environments, such as high-pressure vessels, or require specialized printing machines and materials [11, 65]. Furthermore, current methods lack user-friendly design tools and standardized fabrication workflows suitable for general users, limiting the widespread adoption within HCI and maker communities.

To overcome these challenges and fabricate foamed materials with lattice structure, we propose an accessible, user-friendly fabrication method that leverages conventional FDM 3D printers and commercially available raw materials. Additionally, we provide a design tool that enables users to create customized structures and generate printable models.

3 GYFOAM METHOD

We will present the GyFoam method from three aspects: foam material, lattice structure (Gyroid), and fabrication workflow (basic and optional steps).

3.1 Foam Material

In this study, we developed a new composite foam material composed of TEMs and silicone.

TEM Powder. The foam material (EMH204, SEKISUI CHEMICAL Co., Ltd.)[1] consists of TEMs, with thermoplastic polymer shells encasing low-boiling-point liquid hydrocarbons. According to the manufacturer's specifications, expansion is triggered between 110 to 130°C, with maximum expansion occurring at 160 to 180°C. When heated, the polymer shell softens, and the internal hydrocarbons vaporize, causing the microspheres to expand to 3–4 times their original diameter of 15–40 micrometers.

Base Material. Silicone is widely used for fabricating 3D structures in personal fabrication. Among various types, the Ecoflex series from Smooth-On is particularly popular due to its excellent biocompatibility, elasticity, and stretchability [52, 60]. Taking advantage of its fluidity and moldability, we use Ecoflex 0030 silicone as the base material in our composite to form the initial structures.

The preparation of the TEM-silicone composite will be described in detail in Section 3.3. Notably, incorporating TEMs increases the viscosity of the composite. Moreover, excessively high concentration of the composite contains insufficient silicone, resulting in failed curing. Therefore, we recommend keeping the composite concentration below 40% during fabrication. If the concentration becomes too high, one solution is to add an appropriate amount of silicone oil to improve the fluidity of the composite.

3.2 Gyroid Structure

Although TEMs can achieve substantial expansion, the foaming process often becomes uneven (Fig. 3a) when exposed to heat (Fig. 3a), especially at higher TEM concentrations or in larger parts. If the heating continues until uniform, it may lead to excessive heating of the outer surface. To address this issue, we integrated Gyroid structures with foaming materials, leading to uniform expansion (Fig. 3a) and lightweight structures (Fig. 3b).

Among various lattice structures, Gyroid is a non-intersecting, continuous surface known for its high energy absorption efficiency and large specific surface area [18]. Its well-defined mathematical properties and high degree of parametric controllability make it especially suitable for additive manufacturing. Our research focuses on Gyroid structure and explores a fabrication method that combines foam materials with Gyroid structure.

In GyFoam, the adjustable Gyroid structural parameters include cell size and wall thickness of the Gyroid unit cells (Fig. 4). Due to the precision limitations of 3D printing, there is a constraint relationship between cell size and wall thickness when producing molds (Section 4.3). To avoid printing failures resulting from excessively thin cross-sections, we recommend ensuring that these parameters satisfy a specified Inequality (1). Additionally, our experiments suggest that the wall thickness should exceed 1 mm to achieve complete mold filling.

$$cellsize - 2 \times thickness > 2 \tag{1}$$

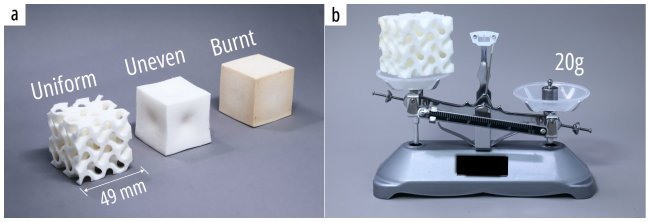

Figure 3: Advantages of the Gyroid Structure: (a) Uniform expansion using GyFoam method; (b) Fabrication of lightweight objects.

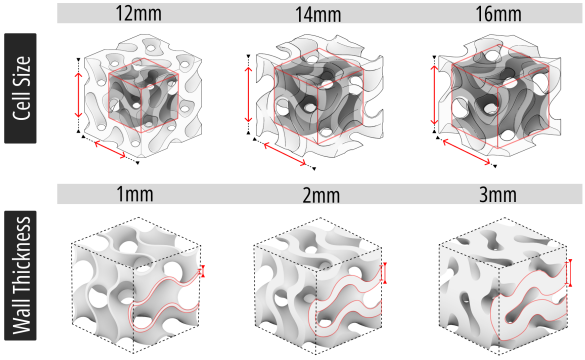

Figure 4: Gyroid structural parameters: cell size and wall thickness.

3.3 Basic Fabrication Workflow

Here, we introduce a basic fabrication workflow (Fig. 5) for Gyroid structures built upon the conventional casting process.

3D printing molds. 3D printing has become a versatile tool for personal fabrication. We use desktop 3D printers (Bambu) with commercially available filaments like PVA (Bambu PVA) and PLA (Bambu PLA) to create molds. The PVA filament, serving as a sacrificial mold material [8, 26], is ideal for fabricating Gyroid structures which cannot be demolded by conventional methods. Users can select either PVA or PLA for mold production based on their demolding needs. When printing with PVA, we recommend a slower printing speed to avoid stringing and adhesion failures that may cause printing defects. Additionally, setting the wall thickness to at least three layers during slicing helps prevent fluid leakage during composite casting.

Casting TEM-silicone composite. Similar to conventional silicone preparation, we mix silicone components A and B with a predetermined amount of TEM, then stir the mixture thoroughly. Once well-mixed, the TEM-silicone composite should be vacuumed

[1]We confirmed that similar expansion effects can be achieved with TEM of other brands, such as 120DU15 (Polychem) and 031DU40 (Expancel).

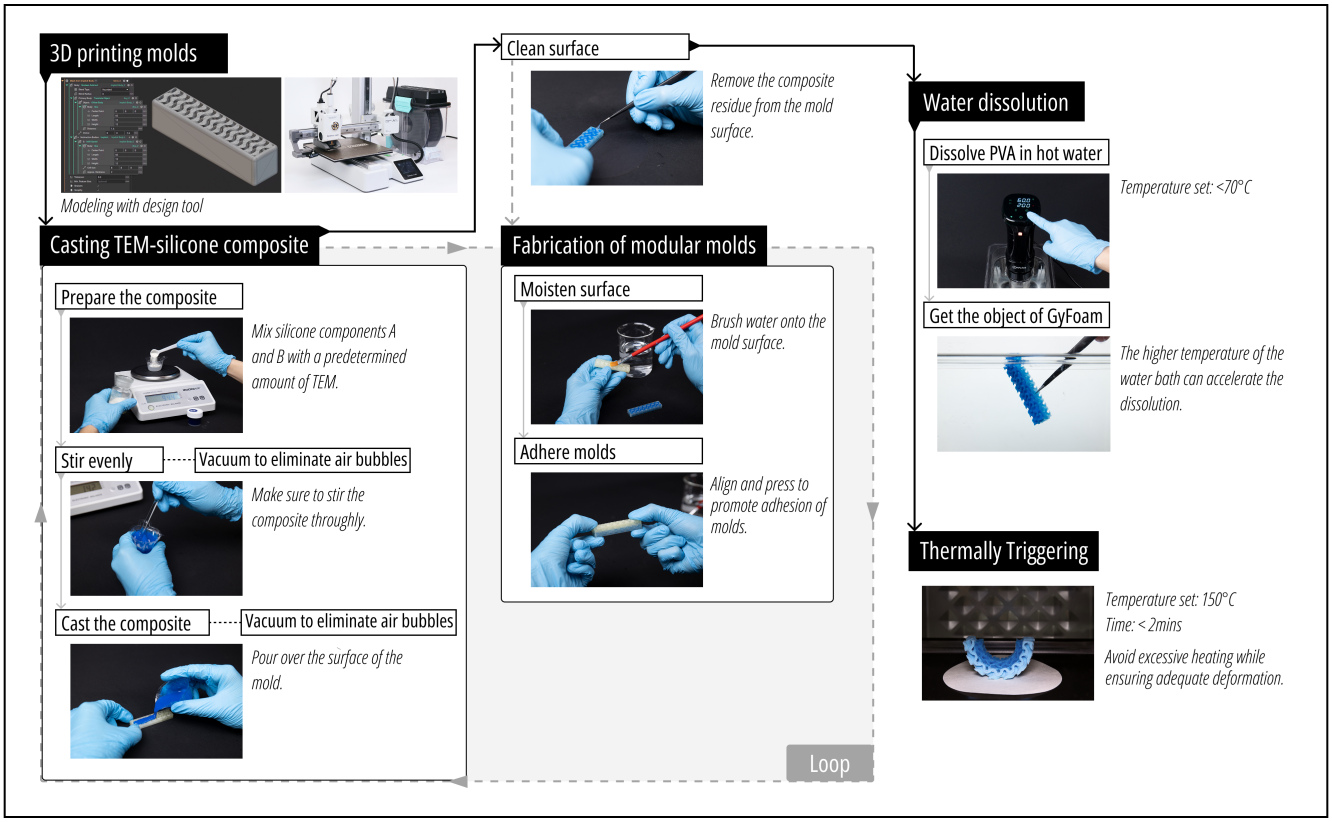

Figure 5: Fabrication Workflow of GyFoam

to eliminate air bubbles. The composite is then poured into the mold cavity and vacuumed again to ensure complete filling and eliminate any residual air bubbles. If the mold is relatively large or has a complex geometry, multiple rounds of casting are recommended to ensure complete coverage. Furthermore, if a specific concentration distribution is desired, we recommend using the "Segmentation Casting" method described in Section 3.5.

After casting, we perform surface post-processing to reduce silicone residue adhering to the mold surface. The filled mold is placed on a level surface to cure. Slightly increasing the temperature (below 70°C) is recommended to accelerate the curing process. Once the silicone has cured, surface treatment of the mold is necessary to remove any residual composite that may have adhered to the surface, facilitating subsequent steps.

Water dissolution. After completing the casting process, we recommend using a water bath maintained at 60°C, with either continuous agitation or ultrasonic vibration (e.g., an ultrasonic cleaner), to effectively accelerate the dissolution of PVA. Additionally, it is advisable to periodically replace the liquid in the container to prevent the concentration of dissolved PVA from becoming too high, which may slow down the dissolution process.

Thermally triggering. Once the mold has fully dissolved, we retrieve the stable TEM-silicone composite, followed by thorough cleaning and drying. The foaming process is then triggered by heating tools such as ovens, thermostatic drying chambers, or heat guns, with a recommended heating temperature of 150°C. Since the expansion occurs so rapidly, we suggest users monitor the process to appreciate the dynamic transformation. During heating, it is advisable to use tools like tweezers to reposition or flip the composite, ensuring uniform heating. Additionally, controlling the heating duration is essential to prevent overheating (Fig. 10b), which could compromise both the aesthetic quality and functional performance of the composite.

3.4 Optional Fabrication Method: Modular Assembly Molds

We propose a modular fabrication method for producing either large or multi-layered objects, where both cases involve assembling multiple molds to construct the final form. We observe that when moistened, the surface of a PVA mold transitions into a viscous, adhesive gel state, allowing it to bond with other PVA or PLA molds and even cured silicone surfaces. By applying a thin layer of water and pressing the molds together, users can easily assemble them with good adhesion (Fig. 6). It is important to keep contact surfaces clean and smooth to promote effective adhesion of the PVA. This method allows for the creation of large, seamless objects without the need for mechanical joints, resulting in higher structural strength and stability.

Following assembly, we proceed with the subsequent "Casting TEM-silicone composite" process. The "Casting TEM-silicone Composite" and "Fabrication of modular molds" steps form a fabrication loop (Fig. 5), continuing until all molds are properly bonded together and completely filled.

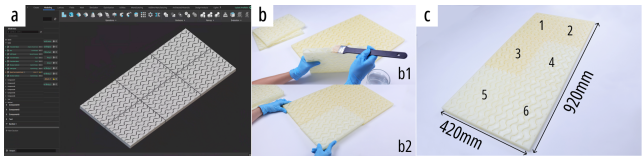

Figure 6: Assembly mold for mattress fabrication: (a) Design molds through our design tool; (b) Using a brush to moisten the mold surfaces along the seams and assembling the modular molds; (c) Waiting for the PVA molds to cure.

3.5 Optional Fabrication Method: Segmentation Casting

For users aiming to achieve a controlled concentration distribution along a planar surface, we recommend using the segmentation casting method. Users can employ 3D-printed barriers to separate regions with varying concentrations (Fig. 7). During fabrication, these barriers are placed on the mold surface, allowing different concentrations of the composite to be poured into designated areas. To prevent unintended mixing or spreading, it is recommended to pour from higher to lower concentrations, as higher-concentration composites have lower fluidity and require more time to fill the mold.

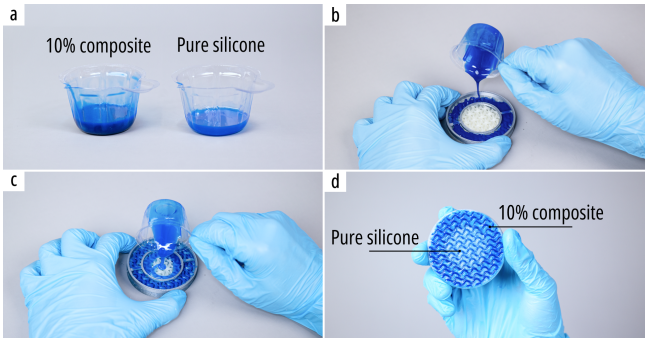

Figure 7: Segmentation casting: (a) Preparation of materials with varying concentrations. (b,c) Sequential casting of materials into designated regions, starting from high concentration to low concentration. (d) Customizable concentration distribution.

4 FOAMING MECHANISM OF GYFOAM

We further explore the foaming mechanism of the TEM-silicone composite from a microscopic perspective. We also demonstrate that it can achieve uniform expansion through the Gyroid structure. Moreover, through a series of experiments, we quantitatively evaluate its expansion capacity.

4.1 Microscopic Characterization of Foaming

In GyFoam, TEMs and silicone form a composite system. Therefore, it is necessary to investigate the foaming mechanism within this composite system.

Materials science research [6, 36] has revealed the expansion behavior of TEMs in substrate materials. After heating, the microspheres undergo significant volumetric expansion, occupying the space originally filled by the substrate. Building on prior work, we further examined the interfacial bonding between composites of different concentrations using scanning electron microscopy (SEM, SU-70, Hitachi, Japan; 150 kV).

From a microscopic perspective, TEMs are uniformly distributed throughout the silicone, with no obvious signs of local agglomeration. SEM images (Fig. 8) also reveal no noticeable gaps or cracks at these bonding interfaces, indicating that the bonding between composites of different concentrations is stable and robust, effectively preserving the overall structural integrity of the composite material.

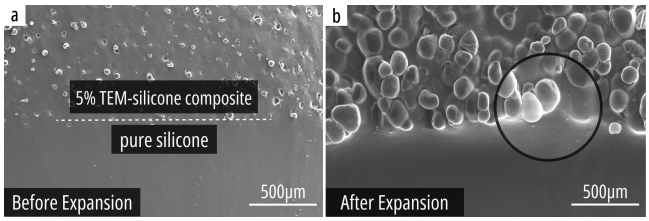

Figure 8: SEM images of 5% TEM–silicone composite bonded with pure silicone, shown (a) before and (b) after foaming.

4.2 Uniform Expansion via Gyroid Structure

To assess the effectiveness of the Gyroid structure in enhancing the uniformity of heating and expansion in TEM-silicone composites, we further conducted a comparative experiment. Building on our initial validation using simple cubic models (Fig. 3a), we extended the study to a more complex and larger 3D geometry—the Stanford Bunny. Three versions of the bunny model (Fig. 9a) were fabricated: a solid structure, a Gyroid-structured version (both filled with 20% TEM-silicone composite), and a pure silicone version, serving as a control.

First, we observed that the solid structure exhibited highly uneven expansion, which compromised shape controllability. A solid bunny-shaped sample was placed in a 150°C oven (Fig. 9b). The outer surface expanded rapidly, resulting in severely irregular deformation. After several minutes of heating, the sample had lost its recognizable contour and appeared heavily distorted. At this point, the embedded temperature sensor indicated that the internal temperature had only reached 63 °C. Continued heating led to noticeable charring on the surface, while the interior remained under-expanded and partially collapsed.

In contrast, the lattice-structured bunny demonstrated uniform appearance after expansion. To further assess the internal expansion uniformity, we performed 3D scanning using the Einscan Pro 2X (Shining 3D, Hangzhou, China), and reconstructed the geometry. Due to the porous nature of the lattice, a complete scan was not

feasible. We therefore cut the sample into two parts (Fig. 9 c1) and scanned the exposed cross section. We extracted approximately corresponding cross-sections from the digital model (Fig. 9 c2) and computed the Euclidean distance between the 3D-scanned and digital models as an error metric. Based on these measurements, an error map (Fig. 9 c3) was generated. The results indicate that the 3D-scanned model aligns closely with the digital model across the cross-sections, demonstrating good uniformity of expansion on both the inner and outer surfaces. Notably, the regions with the largest errors are attributed to significant resistance between the cutting blade and the model, which caused excessive compression and subsequent deformation during the cutting process.

The experiments demonstrate that the Gyroid structure promotes more uniform expansion of this foam material, thereby improving the controllability of the foaming process and laying the groundwork for shape control and mechanical property tuning.

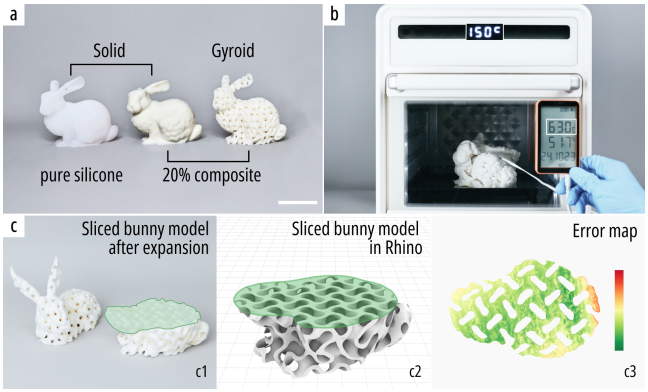

Figure 9: Validation of uniform expansion: (a) Sample models; (b) Heating solid bunny with internal temperature monitoring; (c) Comparison of cross-sections from the 3D-scanned physical model and the digital model, used for error analysis and evaluation of expansion uniformity. Scale bar: 50 mm.

4.3 Controllable Volumetric Expansion

Heating and foaming. The SEM images clearly reveal that the macroscopic expansion of the composite is primarily driven by the thermal expansion of TEMs. To further understand the process, we examined the effect of heating duration (at a constant temperature of 150°C) on the final expansion. The concentration of all samples was 30%. The experimental results (Fig. 10a) indicate that the composite undergoes three distinct stages during heating: "uneven heating, full expansion, overheating." Accordingly, the samples exhibit three phases of deformation: "non-uniform expansion, uniform expansion, shrinkage." Additionally, the color of the samples gradually darkens as the heating time increases. These phenomena occurring during heating are due to the thermal expansion of TEM (Fig. 10b). Once the accumulated thermal energy in the microspheres exceeds their threshold, they rupture, resulting in both volume reduction and color darkening. This insight allows us to optimize heating methods and durations during fabrication, ensuring the creation of objects that are both aesthetically pleasing and functionally effective.

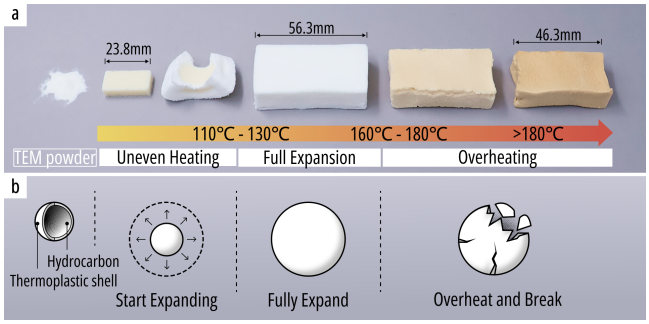

Figure 10: (a) Foaming behavior of the 30% concentration composite under different heating conditions. (b) Basic principle of TEM's thermal expansion.

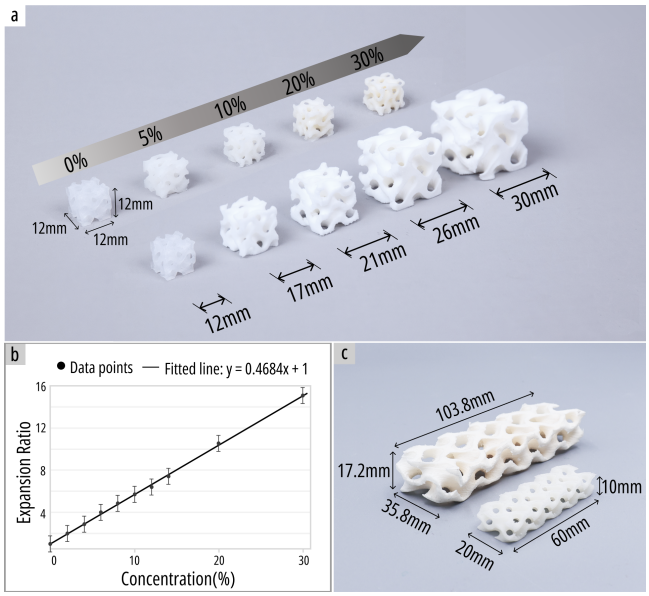

Figure 11: (a) Samples with different concentrations before and after foaming; (b) Experimental results and curve fitting. (c) Isotropic expansion of a rectangular sample.

Volumetric expansion ratio. The most basic characteristic of GyFoam is its volumetric expansion ratio (K), defined as $K = (V1 - V0) / V0$, where $V1$ is the volume after expansion and $V0$ is the initial volume. The concentration of the composite directly influences the expansion ratio. To explore this relationship, we conducted experiments on cubical composite samples with identical dimensions and same Gyroid structural parameters but different concentrations. All samples were heated to achieve full expansion (Fig. 11a). Then we estimated the volume of the samples by measuring their buoyancy using Archimedes' principle. Figure 11b and Equation 2 show a positive correlation between the expansion ratio of the composite and concentration of TEM. The experimental data were fitted to a linear function (Fig. 11b), yielding a coefficient of determination (R^2) of 0.997, indicating a strong correlation. Finally, the accuracy of the model was verified using a sample with an 22% concentration,

resulting in an error of 3.9%. These results confirm the predictive capability of the fitted equation, helping us in the refinement of software parameters to more accurately reflect physical variables.

$$K = 0.468 \times Concentration + 1 \tag{2}$$

Isotropic expansion. To further understand the foaming behavior of GyFoam, we fabricated a rectangular sample with initial dimensions of 60 × 20 × 10 mm and a concentration of 12%. After thermal expansion, the sample exhibited volumetric expansion, with a three-axis expansion ratio of 1.73, 1.79, and 1.72 (Fig. 11c). These results demonstrate that GyFoam enables not only substantial volumetric expansion but also isotropic expansion behavior.

5 CUSTOMIZABLE STIFFNESS OF GYFOAM

The expansion of TEM results in significant changes in the mechanical properties of the composite material of GyFoam. Stiffness, as a fundamental determinant of haptic feedback, significantly influences how users perceive and interact with physical interfaces in HCI. Therefore, we investigate how the stiffness of the foamed composite can be tailored by two tuning variables: the concentration and Gyroid structural parameters (cell size and wall thickness).

We used a universal testing machine (UTM, Instron-5943, Instron, USA) to conduct all tensile and compression tests (Fig. 12a).

5.1 Tuning Variable: Concentration of TEM-silicone Composite

We chose Young's modulus to characterize the effect of composite concentration on the material after foaming.

Following the ISO 37:2005 standard, we prepared dumbbell-shaped samples with a concentration gradient of 3%, producing three samples for each concentration. We conducted tensile tests to measure the Young's modulus. To ensure data reliability, we took multiple measurements for each sample group to minimize random and systematic errors. Additionally, we observed that as the concentration increased, the samples exhibited more pronounced plastic deformation and became less capable of returning to their original shape after stretching.

The stress-strain curves for samples of different concentrations are shown (Fig. 12b, left), illustrating their tensile performance and corresponding force feedback. Notably, the curve for samples with an 18% concentration exhibits a sudden change due to fracture during the tensile test.

After processing the experimental data, we obtained the quantitative relationship between concentration and Young's modulus (Fig. 12b, right). The results show a positive correlation between the concentration of TEM and Young's modulus, meaning that the material becomes stiffer and more resistant to tensile forces as concentration increases. Further data fitting, as shown in Equation 3, yielded a coefficient of determination (R^2) of 0.990, indicating a high level of fit. This establishes a clear relationship between the Young's modulus and concentration for this new composite material.

$$E_{solid} = 1.030 \times 10^7 \times Concentration + 9.428 \times 10^4 \tag{3}$$

5.2 Tuning Variable: Structural Parameters of Gyroid Lattice

In the fields of mechanical engineering and materials science, lattice structural parameters can have a profound impact on physical properties [24]. Therefore, we investigated the impact of Gyroid structural parameters on the stiffness of foamed composites.

We conducted experiments by varying two key parameters: cell size and wall thickness (Fig. 4). For all samples, the concentration of the TEM-silicone composite was kept at 12%. The details of the two experimental sets are as follows.

- The first set of experiments examined the effect of cell size on stiffness. The wall thickness was fixed at 2 mm, with cell sizes set to 4 mm, 6 mm, 8 mm, 10 mm, and 12 mm.
- The second set of experiments investigated the effect of wall thickness on stiffness. The cell size was fixed at 10 mm, while the thickness varied across 2 mm, 3 mm, 4 mm, and 5 mm.
- Notably, due to the conflict between size and thickness, the samples with a wall thickness of 5 mm and a cell size of 4 mm resulted in a fully filled solid cube rather than a Gyroid structure.

After foaming, we performed compression tests on the samples. The results of these two experiments are illustrated in Figure 12c, revealing how Gyroid structural parameters influence overall stiffness. Specifically, cell size is negatively correlated with stiffness, while wall thickness is positively correlated with stiffness. By adjusting Gyroid structural parameters, we can effectively tailor the stiffness of the TEM-silicone composite after foaming. We now introduce additional variables, allowing stiffness tuning to be independent of the composite's volumetric expansion which is determined by material concentration.

5.3 Stiffness Model Fitting and Evaluation

To better meet users' customization needs, and based on prior studies [24, 33], we developed a stiffness model derived from the above experiments. This model[2] (Equation 4) provides an approximate stiffness of the TEM-silicone composite after foaming, based on material concentration and Gyroid structural parameters. To validate the accuracy of the predictive model, we fabricated a sample set with a concentration of 15%, a cell size of 12 mm, and a wall thickness of 3.6 mm. The measured stiffness coefficient of this sample was 11.28 N/mm, while the predicted stiffness coefficient was 10.67 N/mm, with an error of 5.7%. This demonstrates that our predictive model has a good rigidity prediction performance.

$$S_* = 2.52 \times E_{Solid} \times \left(\frac{thickness}{cellsize}\right)^{1.7} \times L \tag{4}$$

6 MORPHING STRUCTURES

When creating 3D shapes, additional material may be required to print support structures for molds, resulting in material waste. To enhance manufacturing efficiency and fully exploit GyFoam's potential, we drew inspiration from studies on shape-changing interface [45] and programmable material [57], such as 4D printing

[2] In this equation, S_* represents predicted stiffness (N/m), E_{Solid} represents Young's modulus (Pa) of material under selected concentration, L represents the length (m) of the boundingbox of the sample.

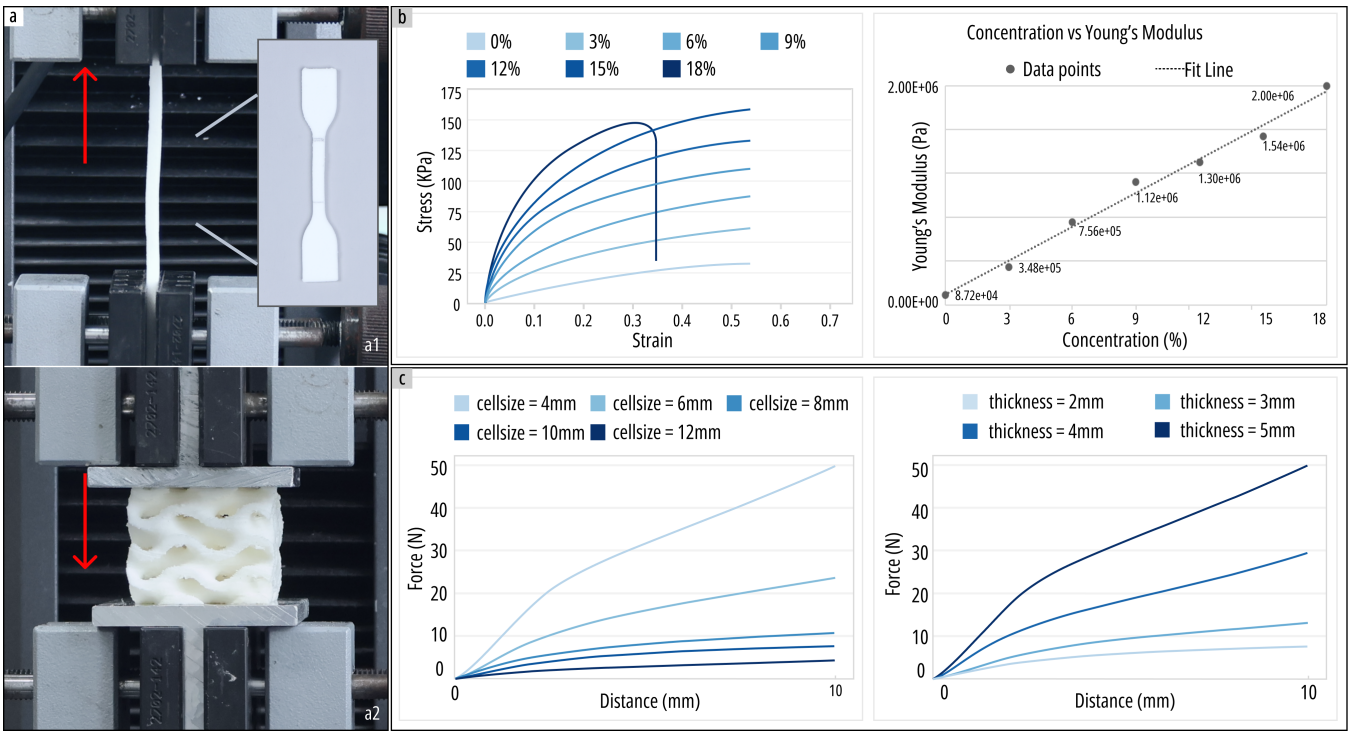

Figure 12: (a) Mechanical testing setup, including tensile and compression tests with corresponding samples; Experimental results and data visualization of (b) tensile and (c) compression tests.

[3, 58]. In GyFoam, the strain mismatch between composites of different concentrations after expansion generates internal stresses, which in turn drive overall deformation. Additionally, materials with different concentrations are tightly bonded (Section 4.1) to ensure effective force transfer. Building on this principle, we propose three shape control strategies for GyFoam: (1) bilayer-induced bending, (2) concentric-induced wavy edges, and (3) concentric-induced internal doming. A library of morphing structures is presented in Figure 13 to show the shapes produced by these deformation control strategies. Additionally, we conducted preliminary simulations to explore the controllability and predictability of these deformations.

Bilayer-induced bending. This deformation strategy leverages a bilayer structure composed of two foam layers with different material concentrations. The mismatch in expansion between the two layers generates an internal bending moment, resulting in predictable out-of-plane deformation. Our deformation library demonstrates how varying the concentration of the active layer affects the resulting bending curvature.

Concentric-induced wavy edges. We present a structure in which the inner ring has a lower composite concentration, while the outer ring has a higher concentration. During expansion, the outer ring is constrained and stretched by the inner ring, resulting in periodic wavy edges. By adjusting the composite concentrations and geometric dimensions, we can achieve wavy edges with varying amplitudes and wave counts.

Concentric-induced internal doming. In contrast to wavy edges, internal doming is achieved by reversing the concentration distribution. The inner region, with its higher expansion capability, is constrained by the surrounding structure, preventing lateral expansion and instead forcing upward deformation into a dome shape. Our library showcases various internal doming effects resulting from different concentration gradients, illustrating a diverse range of dome heights and shapes.

7 DESIGN TOOL

To accommodate users' personalized and diverse needs, we have developed design tools deployed across two software platforms. For novice users, we established a tool based on Rhino and Grasshopper, with HumanUI serving as the user interface (Fig. 14a, b). This tool enables users to model simple geometries and preview basic deformation effects by adjusting geometric parameters. For more advanced users and requirements, we developed a modeling assistant based on nTop [42], which enables more complex structural designs and facilitates optimized mold generation (Fig. 14c, d). All the models presented in this study were created using the design tool we developed.

Building on the design software platforms, we also developed online documentation[3] to help users better understand the modeling workflow. The documentation includes design templates and reference files intended to support and guide users in their modeling process.

[3] https://gyfoam.github.io/

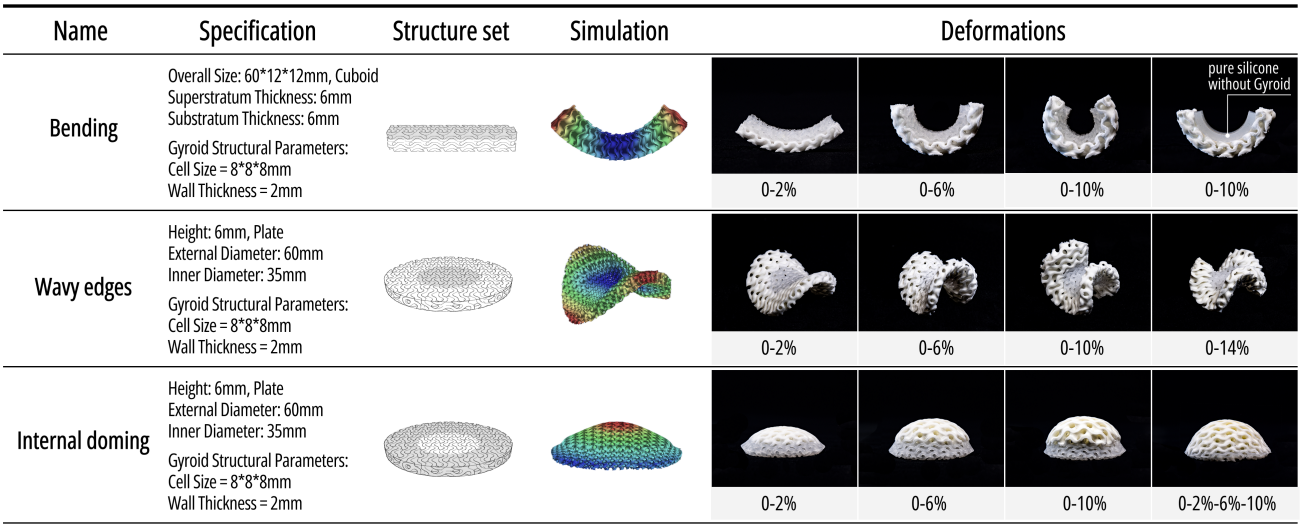

Figure 13: GyFoam Morphing Library: three morphing structures—bending, wavy edges, and internal doming.

7.1 User Interface of Rhino

Select or Import. Users can begin by choosing from our predefined base models (Fig. 14a), which are closed polygon surfaces serving as the bounding box for lattice structure. Experienced 3D modeling users with specific designs can also freely import their own closed polygonal objects, such as STL files.

Customize Gyroid Structure and Material Concentration. To design suitable Gyroid structures and achieve desired deformation, users can adjust the global parameters of Gyroid structure (Fig. 14a), including cell size and wall thickness. According to the guidelines we established in Section 3, these two parameters should satisfy Inequality (1). Additionally, users can specify the concentration of TEM-silicone composite.

Preview and Export. To facilitate a comprehensive understanding of GyFoam before real fabrication, the design tool allows users to preview the deformation based on the selected model (Fig. 14 b3). If users modify structural parameters or material concentration, they need to refresh the tool to visualize the updated deformation. Finally, users can preview and export the mold model files (Fig. 14 b4), which can then be imported into 3D printing slicing software for further processing.

7.2 Advanced Modeling of nTop

nTop is a specialized software designed for lattice structure modeling. We have developed a suite of design assistance tools and modeling templates. While its modeling logic and workflow are similar to those of Rhino and Grasshopper, nTop offers significantly faster computation and a more efficient lattice modeling process when handling complex designs. Beyond conventional modeling (Fig. 14 d1, d2), we utilized nTop to develop two advanced modeling techniques: gradient Gyroid modeling (Fig. 14 d3) and eggshell-structured mold modeling (Fig. 14 d4). Similarly, nTop can also export mold model files for 3D printing. We have open-sourced the corresponding modeling template files in the online documentation[4] to better assist users.

Gradient Gyroid modeling. Research in mechanical engineering has shown that lattice structures with gradient variations exhibit enhanced mechanical properties [25]. We implemented the design and modeling of such gradient Gyroid structures in nTop and provided a sample file to help users better understand the process and support their own modeling efforts.

Eggshell-structured mold modeling. We optimized the mold structure by drawing inspiration from the eggshell fabrication method [4]. This approach significantly reduces PVA consumption by creating thin-walled molds instead of fully filled ones. Additionally, the thin PVA layer produced by the eggshell method greatly increases the contact area exposed to water during dissolution, substantially accelerating the dissolution process. Users can refer to the provided sample file to decide whether the eggshell method is suitable for their mold fabrication needs. We recommend using this method when the model is relatively large.

8 APPLICATION

To illustrate the potential of GyFoam for prototyping and tangible interaction, we designed and produced several applications: large products of personal fabrication, wearable products, and soft tangible interfaces. All applications were developed using the design tool we provided. We have also made the detailed modeling configurations and model files open-source[5] to better support users in their creation process.

8.1 large products of personal fabrication

8.1.1 Scaled-Up Bunny Sculpture. We fabricated relatively large bunny sculptures that exceed the build volume of the desktop 3D

[4]https://gyfoam.github.io/pages/subpage/designtool.html
[5]https://gyfoam.github.io/pages/subpage/application.html

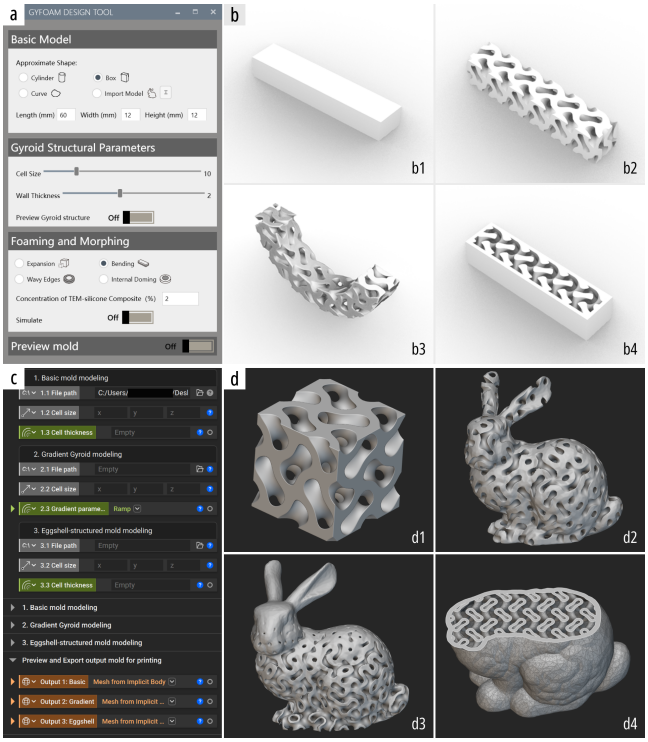

Figure 14: Design tool of GyFoam: (a) Grasshopper interface. (b) Grasshopper Workflow: selecting the basic model, setting structural parameters and previewing Gyroid structure, visualizing deformation, and generating the mold model. (c) nTop interface. (d) nTop examples: Gyroid cube, Gyroid Bunny with uniform thickness, Gyroid Bunny with gradient thickness, and eggshell-structured mold of the Gyroid Bunny.

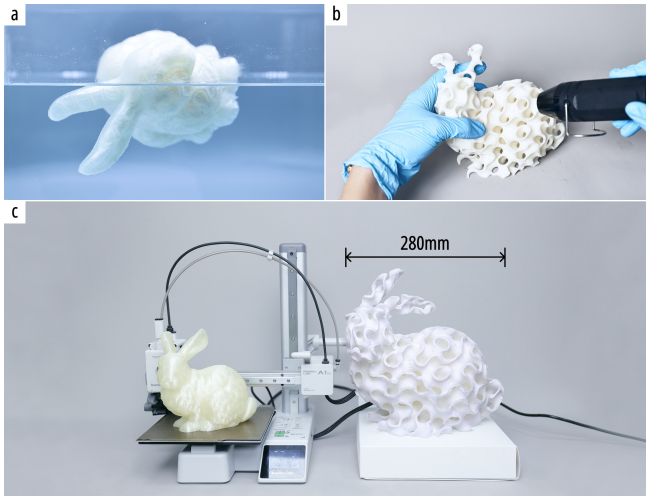

Figure 15: GyFoam bunny: (a) Dissolving the PVA mold; (b) Triggering expansion using a heat gun; (c) Fabricating a large bunny sculpture that exceeds the build volume of the 3D printer used for mold fabrication.

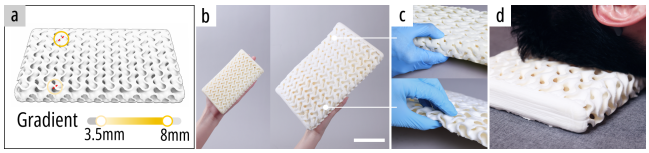

Figure 16: GyFoam pillow: (a) Constructing the pillow with a wall thickness gradient using our design tool; (b) Expanding to a single-person pillow; (c) Varying stiffness between the two sides; (d) Allowing users to rest on the preferred side based on desired firmness. Scale bar: 100 mm.

printer (Bambu A1 mini) used to produce the initial PVA molds. Although the molds were entirely printed within the printer's limited build area, the final sculpture expanded significantly after heating, exceeding the build volume of the original printer. Our method allows the fabrication of large, soft objects that are free from assembly seams, which are often unavoidable when using traditional 3D printing approaches such as directly printing with flexible TPU within limited build volumes. This demonstrates the potential of our method for producing oversized aesthetic forms in domains such as art, education, and exhibition design.

8.1.2 Gradient-stiffness Pillow. We developed a pillow with a built-in gradient of softness and firmness. Using our design tool, we implemented a gradual change in wall thickness within the lattice structure (Fig. 16a), enabling the creation of a smooth stiffness gradient across the pillow. Initially measuring 12 × 7 × 1.4 cm, the pillow expands to 30 × 18 × 3.5 cm when heated (Fig. 16b). This enables personalized comfort—users can rest on the firmer side for enhanced neck support, or on the softer side for a more cushioned, enveloping feel (Fig. 16c, d).

8.1.3 Customizable Single Mattress. Conventional mattresses typically use uniform materials and structures, making it difficult to provide localized support. Moreover, producing customized mattresses to meet personalized needs—whether through traditional manufacturing or emerging 3D printing [1]—remains costly. To demonstrate GyFoam's scalability and customization capabilities, we fabricated a twin-sized mattress that expands to approximately 0.8 m × 1.8 m after heating, using a mold assembled from six modular sections 6. With our design tool, users can customize the shape and size of the mattress to suit individual preferences. Additionally, by adjusting the lattice structure with design tool or modifying material concentrations during fabrication, users can control the local stiffness to accommodate specific comfort and support requirements.

8.2 Wearable Products

8.2.1 Midsoles with Gyroid Structure. Leveraging GyFoam's ability to customize stiffness and deformation, we fabricated lattice-structured shoe midsoles. Sharing similarities with those presented in previous work [11, 71], our approach extends this idea by demonstrating that midsoles with diverse sizes, curvatures, and softness

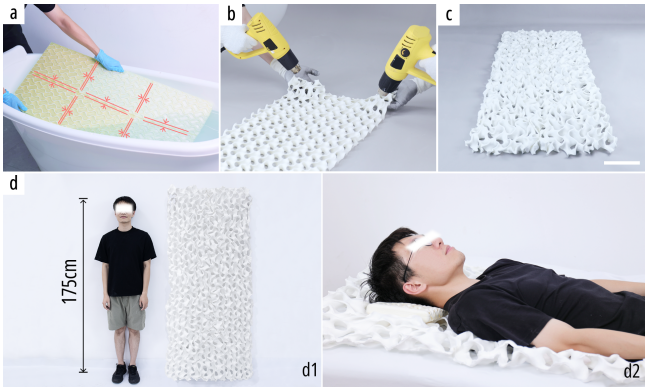

Figure 17: GyFoam mattress: (a) Dissolving the mold in a large container; (b) Heating with heat guns while wearing heat-resistant gloves; (c) Expanded form after heating; (d) Serving as a supportive and comfortable single mattress. Scale bar: 200 mm.

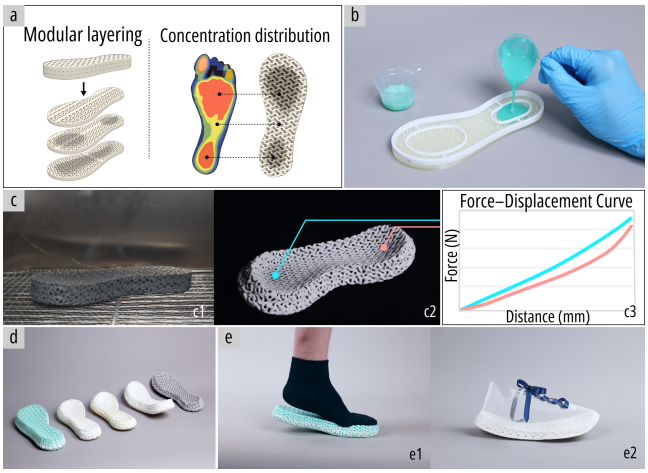

Figure 18: GyFoam midsoles: (a) Midsole design details; (b) Segmentation casting to control concentration distribution; (c) Foaming process and programmable stiffness; (d) Midsoles with different shape and size fabricated from the same mold; (e) Wearing tests.

levels can be fabricated using a single set of molds. Specifically, to achieve localized differences in stiffness, we designed region-specific material concentrations based on plantar pressure distribution to match varying support needs. In fabrication, we adopted a segmentation casting approach by dividing the mold into sections and injecting foaming mixtures with different concentrations accordingly. From a shaping perspective, we employed a modular, layered casting technique, where differences in concentration between layers induced curvature in the final structure. In preliminary wear tests, users reported a high level of comfort, attributed to the midsole's effective shock absorption. We hope this method will empower makers to produce personalized footwear and inspire future applications in areas such as foot care and orthopedic support.

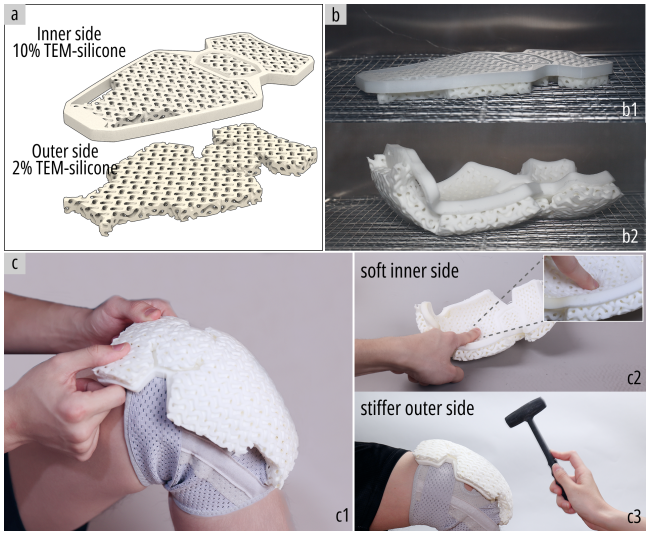

Figure 19: GyFoam Kneepad: (a) Varying concentration across layers; (b) Expanding and morphing to 3D shape; (c) A kneepad with a soft inner surface for comfort and a stiffer outer shell for impact resistance.

8.2.2 Tailored Cushioning Kneepad. We developed a kneepad that transforms from a flat sheet into a three-dimensional shape conforming to the human knee (Fig. 19b). Designed for both comfort and protection, the kneepad features a soft inner layer that rests against the skin and a stiffer outer layer that absorbs external impact (Fig. 19c). To achieve this stiffness gradient, we varied the material concentration across layers—lower on the inner side and higher on the outer side (Fig. 19a). This concentration difference also contributed to the curved shape of the final structure, as the asymmetric expansion between layers induced bending during heating. This flat-to-curved, dual-stiffness kneepad exemplifies GyFoam's advantages in personalized fabrication. At the same time, its flat-to-curved transformation highlights the material's potential for reducing transportation volume and cost, making it valuable for portable or field-deployable scenarios.

8.3 Soft Tangible Interfaces

8.3.1 Interactive Gyroid Lamp. In response to the increasing demand for safe, comfortable, and expressive interactive materials, we developed a flexible Gyroid-structured lampshade using TEM-silicone composite with GyFoam method(Fig. 20). The structure expanded uniformly during fabrication, resulting in a smooth, continuous surface that preserves the geometric beauty of the Gyroid design. Users can switch light colors by tapping the surface and adjust brightness through gentle squeezing (Fig. 20c)—interactions made possible by the soft, deformable nature of the composite material. The lattice design not only enables localized compliance for interaction, but also diffuses light evenly to create a warm and aesthetically pleasing visual effect.

8.3.2 Modular Gaming Keyboard. We developed a modular gaming keyboard (Fig. 21) featuring four directional buttons and a central

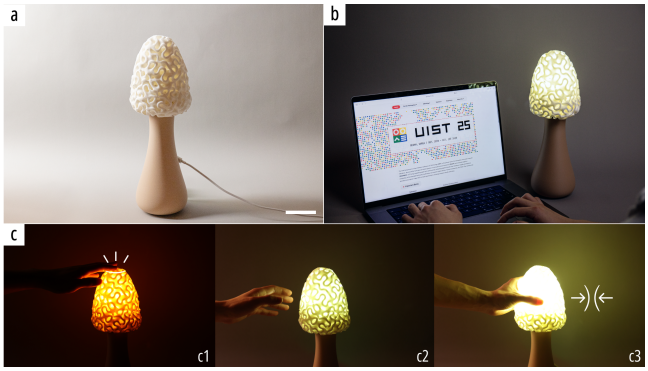

Figure 20: GyFoam lamp: (a,b) The design and application scenario of the interactive lamp; (c) Hand-based interaction for light color switching and brightness adjustment. Scale bar: 50 mm.

hemispherical button. Each button module was independently fabricated using different lattice parameters or deformation strategies. The directional buttons vary in stiffness, achieved by adjusting wall thickness and cell size, enabling nuanced control of actuation force. The hemispherical button employs the internal doming strategy and exhibits monostable behavior, maintaining a raised shape after deformation. This structural design delivers a spring-like, responsive interaction without the need for rigid internal components. The swappable modules allow users to customize force feedback based on gameplay preferences, demonstrating GyFoam's potential for creating physically reconfigurable input devices with tunable mechanical responses.

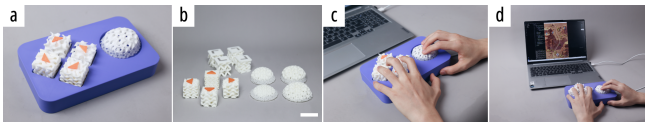

Figure 21: GyFoam keyboard prototype with replaceable key modules, allowing customization of stiffness and force feedback. Scale bar: 40 mm.

9 DISCUSSION, LIMITATION, AND FUTURE WORK

9.1 Fabrication Trade-offs: Time and Material Cost

The GyFoam fabrication process involves multiple steps—including 3D printing sacrificial molds, casting silicone composites, and dissolving the molds—which inevitably increase time and material consumption to the workflow. Compared to fully integrated or additive-only fabrication methods, this approach introduces a degree of complexity and resource overhead. We recognize this as a practical limitation of the current implementation.

However, this trade-off allows for capabilities that are challenging to achieve through simpler fabrication methods. In particular, the combination of foam expansion and lattice structure enables controllable volumetric deformation and programmable stiffness within a larger design space.

To reduce fabrication effort and cost, we have implemented several optimizations. The "eggshell" mold strategy minimizes printing time and PVA usage, while increased curing temperatures accelerate both silicone solidification and mold dissolution. Material cost can also be adjusted based on specific needs: while high-fidelity results can be achieved using premium silicone and microspheres, similar expansion behaviors are attainable with lower-cost alternatives, albeit with potential variation in quantitative behavior.

In future work, we aim to explore direct 3D printing of silicone-based composites as a means to simplify the fabrication process and reduce material waste. Existing liquid-based printing techniques [14, 64] offer promising avenues for fabricating soft and expandable structures without the need for sacrificial molds. By adopting such techniques, it may be possible to print the TEM-silicone composite in a single integrated step, reducing cost and improving precision, repeatability, and accessibility.

9.2 Error Analysis of GyFoam's quantitative relationships

Through experiments, we have established a quantitative relationship between the expansion ratio and the concentration, and proposed a stiffness prediction model. However, these relationships are subject to certain variable limitations, such as the concentration being below 40%, and constraints between cell size and wall thickness. Additionally, since these quantitative relationships are derived from experimental data, they are subject to experimental errors, which are influenced by the fabrication process. For example, residual air bubbles in the mold and composite during production can significantly affect stiffness. The precision of the mold and the accuracy of the composite formulation also impact the final expansion rate and stiffness, placing higher demands on the operator's skill and attention to detail.

Nevertheless, we believe that the empirical models we have proposed are highly valuable for users in understanding the GyFoam method and assisting in model creation. At the same time, we are continuing to conduct more rigorous experiments to develop physical models that better reflect real-world conditions. We will update this model in our online documentation.

9.3 Design Tool Evaluation and Improvements

Compared to other computational software with advanced reverse-design capabilities [15, 41], GyFoam currently provides basic design tools, enabling users to generate mold models and preview simple deformation effects. It should be noted that the deformation previews offered by our Grasshopper-based implementation are not physics-based simulations, but rather geometric approximations meant for intuitive exploration and learning purposes.

Due to the porous structure and limitations in scanning accuracy, we adopted a visual comparison between photographs of the physical model and the simulation result (Fig. 22). The comparison shows that, although certain geometric deviations appear in local details—such as expansion areas and junctions with varying material concentrations—the overall deformation trend and magnitude align well with the simulation prediction.

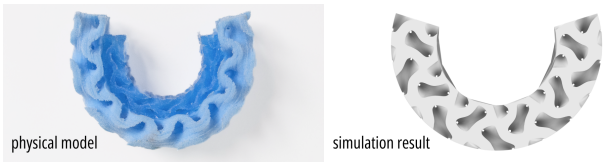

Figure 22: Evaluation of simulation of our design tool.

Meanwhile, in Figure 13, we employed ANSYS to conduct physics-based simulations, which validated the effectiveness of FEA platforms in predicting deformation outcomes. This experience highlights the potential of integrating such simulations into GyFoam in future work. However, due to the highly complex and mesh-dense nature of Gyroid structure, running full-scale finite element simulations on these models presents significant computational challenges, making real-time feedback [67] impractical with current resources.

9.4 Other Lattice Structures Fabricated by GyFoam Method

GyFoam primarily focuses on the Gyroid lattice structure, but our fabrication method is versatile enough to produce other lattice types as well (Fig. 23). Different lattice structures exhibit distinct mechanical properties and advantages, making them suitable for various applications. In the future, we aim to expand our research by exploring and integrating diverse lattice structures to design more complex and customized architectures, tailored to meet a broader range of mechanical performance requirements.

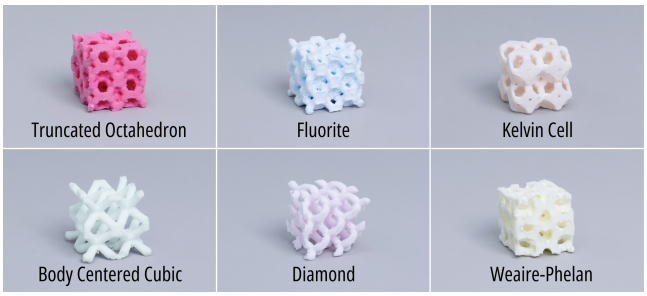

Figure 23: Other six types of lattice structure fabricated via GyFoam method.

9.5 Fatigue Behavior

To evaluate fatigue performance, we conducted 600-cycle compression tests at 10% and 50% strain levels. Over repeated cycles, we observed progressive collapsed height and increased stiffness, which gradually stabilized. Additionally, samples subjected to lower strain exhibited less fatigue. We attribute the height loss to plastic deformation, which prevents full recovery and increases density, resulting in higher stiffness. During fabrication, we also observed a tension between stiffness and fatigue resistance: increasing material concentration improves stiffness but reduces resistance to long-term cyclic loading. Rather than prescribing a fixed solution, we encourage users to explore different concentration settings based on their specific needs.

Finding the right balance between stiffness and durability remains an open and meaningful challenge—especially in interactive scenarios. While our current approach offers tunable mechanical properties through material concentration and structural design, further exploration is needed to refine these parameters for different usage contexts. Future work may also investigate multi-material strategies to better accommodate the evolving demands of interactive systems over time.

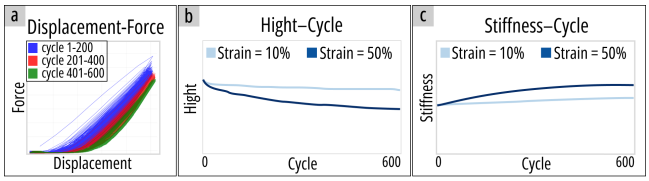

Figure 24: (a) Force–displacement curves over 600 compression cycles at 10% strain; (b,c) Changes in height and stiffness of samples during cyclic compression tests at 10% and 50% strain.

9.6 Quality of Final Objects

The quality of the final product is influenced by the precision of the mold and the fabrication process.

In our approach, some imperfections are unavoidable, such as the surface texture resulting from 3D-printed molds. During the curing process, the TEM-silicone composite precisely replicates the mold's surface patterns. To minimize this effect, we recommend using finer printing settings, such as reduced layer height. This improves mold resolution and enhances the overall quality of the final product.

Meanwhile, some efforts in fabrication can significantly improve product quality. In Section 4.3, we outline a detailed fabrication workflow with practical recommendations for achieving high-quality results. By following these guidelines and maintaining precision, users can quickly gain proficiency and reduce imperfections. However, we also view these "imperfections" as opportunities for personalized expression and the creation of more diverse and unexpected forms.

9.7 Safety Issue

Safety considerations are essential throughout the fabrication process, particularly when handling silicone, TEM powder, and high-temperature equipment. To minimize health risks, operators should wear appropriate personal protective equipment, including masks and gloves, to prevent direct contact with materials and avoid inhaling airborne particles.

Additionally, the foaming process requires exposure to high temperature. During this stage, operators should take precautions to avoid burns or other injuries from direct contact with heated objects, such as TEM-silicone composites or heating devices. It is advisable to use tools like tweezers or heat-resistant gloves.

10 CONCLUSION

In this paper, we present **GyFoam**, a fabrication approach for fabricating foam material that enables controlled and uniform expansion.

Leveraging standard 3D printers and commercially available materials—printing filaments, thermo-expandable microspheres, and silicone—GyFoam enables the creation of expandable objects with high-quality shapes and customizable stiffness. Our experiments reveal two primary strategies for customizing stiffness: adjusting material concentration and modifying lattice structural parameters. To support diverse form factors, we propose three shape-control strategies: bending, wavy edges, and internal doming. We also present an intuitive design tool that allows users to configure lattice parameters, preview basic deformations, and generate printable mold models. Through a series of application scenarios, we demonstrate GyFoam's versatility in personal fabrication of large objects and wearable products, interactive flexible interfaces, and aesthetic designs. We aim to empower designers, makers, and researchers with an accessible approach to fabricating soft objects with tailored shapes and mechanical properties.

Acknowledgments

This project was supported by the National Natural Science Foundation of China under Grant No. 62472371 and Grant No. T2422021.

The authors would also like to thank all the reviewers for their insightful and constructive opinions; Zhiyuan Zhou and Yuchen Wang for their efforts and inspiring suggestions during the early-stage exploration of this work; Sibo Zhou for the assistance in preparing supplementary materials during the revision process.

References

[1] 3D-Printing Mattress 2025. *Example of customizable Mattress by 3D printing.* https://www.youtube.com/watch?v=G05XGncJP7c

[2] Diab W Abueidda, Mohamed Elhebeary, Cheng-Shen Andrew Shiang, Siyuan Pang, Rashid K Abu Al-Rub, and Iwona M Jasiuk. 2019. Mechanical properties of 3D printed polymeric Gyroid cellular structures: Experimental and finite element study. *Materials & Design* 165 (2019), 107597.

[3] Byoungkwon An, Ye Tao, Jianzhe Gu, Tingyu Cheng, Xiang'Anthony' Chen, Xiaoxiao Zhang, Wei Zhao, Youngwook Do, Shigeo Takahashi, Hsiang-Yun Wu, et al. 2018. Thermorph: Democratizing 4D printing of self-folding materials and interfaces. In *Proceedings of the 2018 CHI conference on human factors in computing systems*. 1–12.

[4] Joris Burger, Ena Lloret-Fritschi, Fabio Scotto, Thibault Demoulin, Lukas Gebhard, Jaime Mata-Falcón, Fabio Gramazio, Matthias Kohler, and Robert J Flatt. 2020. Eggshell: ultra-thin three-dimensional printed formwork for concrete structures. *3D Printing and Additive Manufacturing* 7, 2 (2020), 48–59.

[5] Jie-Hua Cai, Ming-Lu Huang, Xu-Dong Chen, and Ming Wang. 2021. Thermo-expandable microspheres strengthened polydimethylsiloxane foam with unique softening behavior and high-efficient energy absorption. *Applied Surface Science* 540 (2021), 148364.

[6] Jie-Hua Cai, Jie Li, Xu-Dong Chen, and Ming Wang. 2020. Multifunctional polydimethylsiloxane foam with multi-walled carbon nanotube and thermo-expandable microsphere for temperature sensing, microwave shielding and piezoresistive sensor. *Chemical Engineering Journal* 393 (2020), 124805.

[7] Xiaofeng Chi, Yuanbo Cai, Liwei Yan, Zhengguang Heng, Chuxiang Zhou, Huawei Zou, and Mei Liang. 2023. Flexible thermal protection polymeric materials with self-sensing and self-adaptation deformation abilities. *ACS Applied Materials & Interfaces* 15, 12 (2023), 15986–15997.

[8] Hojung Choi, Joohoon Kim, Wonjoong Kim, Junhwa Seong, Chanwoong Park, Minseok Choi, Nakhyun Kim, Jisung Ha, Cheng-Wei Qiu, Junsuk Rho, et al. 2023. Realization of high aspect ratio metalenses by facile nanoimprint lithography using water-soluble stamps. *PhotoniX* 4, 1 (2023), 18.

[9] Desktop Metal 2022. *FreeFoam material.* https://www.desktopmetal.com/resources/free-foam

[10] Shuyue Feng, Cheng Yao, Weijia Lin, Jiayu Yao, Chao Zhang, Zhongyu Jia, Lijuan Liu, Masulani Bokola, Hangyue Chen, Fangtian Ying, et al. 2023. MechCircuit: Augmenting Laser-Cut Objects with Integrated Electronics, Mechanical Structures and Magnets. In *Proceedings of the 2023 CHI Conference on Human Factors in Computing Systems*. 1–15.

[11] Haoyu Gao, Xianmei Huang, Abilash Rosario Arockiyasamy, Xuan Zhou, Xiaohong Ding, Longhui Zheng, Yilong Liu, Fuquan Ye, Zixiang Weng, and Lixin Wu. 2025. Vat photopolymerization of stretchable foam with highly entangled and crosslinked structures. *Nature Communications* 16, 1 (2025), 1–11.

[12] Jianzhe Gu, Yuyu Lin, Qiang Cui, Xiaoqian Li, Jiaji Li, Lingyun Sun, Cheng Yao, Fangtian Ying, Guanyun Wang, and Lining Yao. 2022. PneuMesh: Pneumatic-driven truss-based shape changing system. In *Proceedings of the 2022 CHI Conference on Human Factors in Computing Systems*. 1–12.

[13] Harini Bhuvaneswari Gunasekaran, Sathiyanathan Ponnan, Naveen Thirunavukkarasu, Abdelatif Laroui, Lixin Wu, and Jianlei Wang. 2022. Rapid carbon dioxide foaming of 3D printed thermoplastic polyurethane elastomers. *ACS Applied Polymer Materials* 4, 2 (2022), 1497–1511.

[14] Kathleen Hajash, Bjorn Sparrman, Christophe Guberan, Jared Laucks, and Skylar Tibbits. 2017. Large-scale rapid liquid printing. *3D Printing and Additive Manufacturing* 4, 3 (2017), 123–132.

[15] Ehsan Hajiesmaili, Natalie M Larson, Jennifer A Lewis, and David R Clarke. 2022. Programmed shape-morphing into complex target shapes using architected dielectric elastomer actuators. *Science advances* 8, 28 (2022), eabn9198.

[16] Liang He, Huaishu Peng, Michelle Lin, Ravikanth Konjeti, François Guimbretière, and Jon E Froehlich. 2019. Ondulé: Designing and controlling 3D printable springs. In *Proceedings of the 32nd Annual ACM Symposium on User Interface Software and Technology*. 739–750.

[17] Liang He, Xia Su, Huaishu Peng, Jeffrey Ian Lipton, and Jon E Froehlich. 2022. Kinergy: Creating 3D printable motion using embedded kinetic energy. In *Proceedings of the 35th Annual ACM Symposium on User Interface Software and Technology*. 1–15.

[18] Mark Helou and Sami Kara. 2018. Design, analysis and manufacturing of lattice structures: an overview. *International Journal of Computer Integrated Manufacturing* 31, 3 (2018), 243–261.

[19] David W Holmes, Dilpreet Singh, Riki Lamont, Ryan Daley, David P Forrestal, Peter Slattery, Edmund Pickering, Naomi C Paxton, Sean K Powell, and Maria A Woodruff. 2022. Mechanical behaviour of flexible 3D printed gyroid structures as a tuneable replacement for soft padding foam. *Additive Manufacturing* 50 (2022), 102555.

[20] Alexandra Ion, Johannes Frohnhofen, Ludwig Wall, Robert Kovacs, Mirela Alistar, Jack Lindsay, Pedro Lopes, Hsiang-Ting Chen, and Patrick Baudisch. 2016. Metamaterial mechanisms. In *Proceedings of the 29th annual symposium on user interface software and technology*. 529–539.

[21] Alexandra Ion, David Lindlbauer, Philipp Herholz, Marc Alexa, and Patrick Baudisch. 2019. Understanding metamaterial mechanisms. In *Proceedings of the 2019 CHI Conference on Human Factors in Computing Systems*. 1–14.

[22] Fan-Long Jin, Miao Zhao, Mira Park, and Soo-Jin Park. 2019. Recent trends of foaming in polymer processing: A review. *Polymers* 11, 6 (2019), 953.

[23] Hiroki Kaimoto, Junichi Yamaoka, Satoshi Nakamaru, Yoshihiro Kawahara, and Yasuaki Kakehi. 2020. ExpandFab: Fabricating Objects Expanding and Changing Shape with Heat. In *Proceedings of the Fourteenth International Conference on Tangible, Embedded, and Embodied Interaction*. 153–164.

[24] SN Khaderi, VS Deshpande, and NA Fleck. 2014. The stiffness and strength of the gyroid lattice. *International Journal of Solids and Structures* 51, 23-24 (2014), 3866–3877.

[25] S Farajzadeh Khosroshahi, SA Tsampas, and U Galvanetto. 2018. Feasibility study on the use of a hierarchical lattice architecture for helmet liners. *Materials Today Communications* 14 (2018), 312–323.

[26] Chae-Hwan Kim, Hyun-Young Kim, Jun-Ho Kim, and Jaehwan Kim. 2023. 3D printing-based soft auxetic structures using PDMS-Ecoflex Hybrid. *Functional Composites and Structures* 5, 1 (2023), 015006.

[27] Doheon Kim, Joongi Shin, and Daniel Saakes. 2020. Foam Sheets as Material for Fabricating Large and Functional Soft Objects. In *Companion Publication of the 2020 ACM Designing Interactive Systems Conference*. 239–244.

[28] Donghyeon Ko, Jee Bin Yim, Yujin Lee, Jaehoon Pyun, and Woohun Lee. 2021. Designing Metamaterial Cells to Enrich Thermoforming 3D Printed Object for Post-Print Modification. In *Proceedings of the 2021 CHI Conference on Human Factors in Computing Systems*. 1–12.

[29] Marion Koelle, Madalina Nicolae, Aditya Shekhar Nittala, Marc Teyssier, and Jürgen Steimle. 2022. Prototyping soft devices with interactive bioplastics. In *Proceedings of the 35th Annual ACM Symposium on User Interface Software and Technology*. 1–16.

[30] Robert Kovacs. 2021. Human-Scale Personal Fabrication. In *Adjunct Proceedings of the 34th Annual ACM Symposium on User Interface Software and Technology*. 162–165.

[31] Eldy S Lazaro Vasquez, Netta Ofer, Shanel Wu, Mary Etta West, Mirela Alistar, and Laura Devendorf. 2022. Exploring Biofoam as a Material for Tangible Interaction. In *Proceedings of the 2022 ACM designing interactive systems conference*. 1525–1539.

[32] Hsuanling Lee, Yujie Shan, Huachao Mao, and Liang He. 2024. Fluxable: A Tool for Making 3D Printable Sensors and Actuators. In *Adjunct Proceedings of the 37th Annual ACM Symposium on User Interface Software and Technology*. 1–3.

[33] Wooju Lee, Da-Young Kang, Jihwan Song, Jun Hyuk Moon, and Dongchoul Kim. 2016. Controlled unusual stiffness of mechanical metamaterials. *Scientific reports* 6, 1 (2016), 20312.

[34] Jiaji Li, Shuyue Feng, Maxine Perroni-Scharf, Yujia Liu, Emily Guan, Guanyun Wang, and Stefanie Mueller. 2025. Xstrings: 3D Printing Cable-Driven Mechanism for Actuation, Deformation, and Manipulation. In *Proceedings of the 2025 CHI Conference on Human Factors in Computing Systems (CHI '25)*. Association for Computing Machinery, New York, NY, USA, Article 6, 17 pages. doi:10.1145/3706598.3714282

[35] Jiaji Li, Mingming Li, Junzhe Ji, Deying Pan, Yitao Fan, Kuangqi Zhu, Yue Yang, Zihan Yan, Lingyun Sun, Ye Tao, et al. 2023. All-in-one print: Designing and 3D printing dynamic objects using kinematic mechanism without assembly. In *Proceedings of the 2023 CHI Conference on Human Factors in Computing Systems*. 1–15.

[36] Xiaoyan Liu, Yaling Zhang, Yu Su, Chengzhen Geng, Yu Liu, Jiangping He, and Ai Lu. 2024. 4D printing of cellular silicones with negative stiffness effect for enhanced energy absorption and impact protection. *Composites Part B: Engineering* 282 (2024), 111561.

[37] David Melancon, Benjamin Gorissen, Carlos J García-Mora, Chuck Hoberman, and Katia Bertoldi. 2021. Multistable inflatable origami structures at the metre scale. *Nature* 592, 7855 (2021), 545–550.

[38] Michael R Mitchell, Ciera McFarland, and Margaret M Coad. 2023. Soft air pocket force sensors for large scale flexible robots. In *2023 IEEE International Conference on Soft Robotics (RoboSoft)*. IEEE, 1–8.

[39] Kongpyung Moon, Haeun Lee, Jeeeun Kim, and Andrea Bianchi. 2022. ShrinkCells: Localized and Sequential Shape-Changing Actuation of 3D-Printed Objects via Selective Heating. In *Proceedings of the 35th Annual ACM Symposium on User Interface Software and Technology*. 1–12.

[40] Satoshi Nakamaru, Ryosuke Nakayama, Ryuma Niiyama, and Yasuaki Kakehi. 2017. FoamSense: Design of three dimensional soft sensors with porous materials. In *Proceedings of the 30th Annual ACM Symposium on User Interface Software and Technology*. 437–447.

[41] Amirali Nojoomi, Junha Jeon, and Kyungsuk Yum. 2021. 2D material programming for 3D shaping. *Nature communications* 12, 1 (2021), 603.

[42] nTop 2025. *nTop software*. https://www.ntop.com/

[43] Sora Oka, Kazuki Koyama, Tomoyuki Gondo, Yasushi Ikeda, Yoshihiro Kawahara, and Koya Narumi. 2025. Pneumatic Laser Origami: Rapid and Large-Scale Fabrication of Laser-Welded Pouch Motors for Shape-Changing Products. In *Proceedings of the Nineteenth International Conference on Tangible, Embedded, and Embodied Interaction*. 1–12.

[44] Mehmet Ozdemir and Zjenja Doubrovski. 2024. Foam2Form: 4D printing with programmable foaming. In *Extended Abstracts of the CHI Conference on Human Factors in Computing Systems*. 1–8.

[45] Isabel PS Qamar, Rainer Groh, David Holman, and Anne Roudaut. 2018. HCI meets material science: A literature review of morphing materials for the design of shape-changing interfaces. In *Proceedings of the 2018 CHI Conference on Human Factors in Computing Systems*. 1–23.

[46] Sutirtha Roy, Moshfiq-Us-Saleheen Chowdhury, Jurjaan Onayza Noim, Richa Pandey, and Aditya Shekhar Nittala. 2024. HoloChemie-Sustainable Fabrication of Soft Biochemical Holographic Devices for Ubiquitous Sensing. In *Proceedings of the 37th Annual ACM Symposium on User Interface Software and Technology*. 1–19.

[47] Ryota Sakuma, Koya Narumi, Yoshihiro Kawahara, and Takefumi Hiraki. 2024. TactPrint: 3D Printing Lattice-based Tactile Displays with Optimized and Local Vibration. In *Extended Abstracts of the CHI Conference on Human Factors in Computing Systems*. 1–4.

[48] Rei Sakura, Changyo Han, Yahui Lyu, Keisuke Watanabe, Ryosuke Yamamura, and Yasuaki Kakehi. 2023. Lattisense: A 3d-printable resistive deformation sensor with lattice structures. In *Proceedings of the 8th ACM Symposium on Computational Fabrication*. 1–14.

[49] Rei Sakura, Changyo Han, Keisuke Watanabe, Ryosuke Yamamura, and Yasuaki Kakehi. 2022. Design of 3D-Printed Soft Sensors for Wire Management and Customized Softness. In *CHI Conference on Human Factors in Computing Systems Extended Abstracts*. 1–5.

[50] Harpreet Sareen, Udayan Umapathi, Patrick Shin, Yasuaki Kakehi, Jifei Ou, Hiroshi Ishii, and Pattie Maes. 2017. Printflatables: printing human-scale, functional and dynamic inflatable objects. In *Proceedings of the 2017 CHI Conference on Human Factors in Computing Systems*. 3669–3680.

[51] Madlaina Signer, Alexandra Ion, and Olga Sorkine-Hornung. 2021. Developable metamaterials: Mass-fabricable metamaterials by laser-cutting elastic structures. In *Proceedings of the 2021 CHI Conference on Human Factors in Computing Systems*. 1–13.

[52] Lingyun Sun, Yitao Fan, Boyu Feng, Yifu Zhang, Deying Pan, Yiwen Ren, Yuyang Zhang, Qi Wang, Ye Tao, and Guanyun Wang. 2024. MagneDot: Integrated Fabrication and Actuation Methods of Dot-Based Magnetic Shape Displays. In *Proceedings of the 37th Annual ACM Symposium on User Interface Software and Technology*. 1–18.

[53] Lingyun Sun, Jiaji Li, Yu Chen, Yue Yang, Zhi Yu, Danli Luo, Jianzhe Gu, Lining Yao, Ye Tao, and Guanyun Wang. 2021. FlexTruss: A Computational Threading Method for Multi-material, Multi-form and Multi-use Prototyping. In *Proceedings of the 2021 CHI Conference on Human Factors in Computing Systems*. 1–12.

[54] Lingyun Sun, Jiaji Li, Junzhe Ji, Deying Pan, Mingming Li, Kuangqi Zhu, Yitao Fan, Yue Yang, Ye Tao, and Guanyun Wang. 2022. X-Bridges: Designing Tunable Bridges to Enrich 3D Printed Objects' Deformation and Stiffness. In *Proceedings of the 35th Annual ACM Symposium on User Interface Software and Technology*. 1–12.

[55] Lingyun Sun, Deying Pan, Yuyang Zhang, Hongyi Hu, Junzhe Ji, Yue Tao, Shanghua Lou, Boyi Lian, Yitao Fan, Ye Tao, et al. 2024. Touch-n-Go: Designing and Fabricating Touch Fastening Structures by FDM 3D Printing. In *Proceedings of the 2024 CHI Conference on Human Factors in Computing Systems*. 1–14.

[56] Lingyun Sun, Yue Yang, Yu Chen, Jiaji Li, Danli Luo, Haolin Liu, Lining Yao, Ye Tao, and Guanyun Wang. 2021. ShrinCage: 4D printing accessories that self-adapt. In *Proceedings of the 2021 CHI Conference on Human Factors in Computing Systems*. 1–12.

[57] Ye Tao, Yi-Chin Lee, Haolin Liu, Xiaoxiao Zhang, Jianxun Cui, Catherine Mondoa, Mahnoush Babaei, Jasio Santillan, Guanyun Wang, Danli Luo, et al. 2021. Morphing pasta and beyond. *Science Advances* 7, 19 (2021), eabf4098.

[58] Guanyun Wang, Ye Tao, Ozguc Bertug Capunaman, Humphrey Yang, and Lining Yao. 2019. A-line: 4D printing morphing linear composite structures. In *Proceedings of the 2019 CHI Conference on Human Factors in Computing Systems*. 1–12.

[59] Guanyun Wang, Yue Yang, Mengyan Guo, Kuangqi Zhu, Zihan Yan, Qiang Cui, Zihong Zhou, Junzhe Ji, Jiaji Li, Danli Luo, et al. 2023. ThermoFit: thermoforming smart orthoses via metamaterial structures for body-fitting and component-adjusting. *Proceedings of the ACM on Interactive, Mobile, Wearable and Ubiquitous Technologies* 7, 1 (2023), 1–27.

[60] Guanyun Wang, Chenda Zheng, Yanbo Fu, Kuangqi Zhu, Fuyi Lai, Likang Zhang, Mengyang Li, Xiaoyang Wu, Muyi Ren, Yanpei Zheng, et al. 2024. KiPneu: Designing a Constructive Pneumatic Platform for Biomimicry Learning in STEAM Education. In *Proceedings of the 2024 ACM Designing Interactive Systems Conference*. 441–458.

[61] Guanyun Wang, Kuangqi Zhu, Lingchuan Zhou, Mengyan Guo, Haotian Chen, Zihan Yan, Deying Pan, Yue Yang, Jiaji Li, Jiang Wu, et al. 2023. PneuFab: designing low-cost 3D-printed inflatable structures for blow molding artifacts. In *Proceedings of the 2023 CHI Conference on Human Factors in Computing Systems*. 1–17.

[62] Keisuke Watanabe, Ryosuke Yamamura, and Yasuaki Kakehi. 2021. Foamin: A deformable sensor for multimodal inputs based on conductive foam with a single wire. In *Extended Abstracts of the 2021 CHI Conference on Human Factors in Computing Systems*. 1–4.

[63] Dylan Weber and Sriharsha Srinivas Sundarram. 2023. 3D-printed and foamed triply periodic minimal surface lattice structures for energy absorption applications. *Polymer Engineering & Science* 63, 4 (2023), 1133–1145.

[64] Jonathan D Weiss, Alana Mermin-Bunnell, Fredrik S Solberg, Tony Tam, Luca Rosalia, Amit Sharir, Dominic Rütsche, Soham Sinha, Perry S Choi, Masafumi Shibata, et al. 2025. A Low-Cost, Open-Source 3D Printer for Multimaterial and High-Throughput Direct Ink Writing of Soft and Living Materials. *Advanced Materials* (2025), 2414971.

[65] David M Wirth, Anna Jaquez, Sofia Gandarilla, Justin D Hochberg, Derek C Church, and Jonathan K Pokorski. 2020. Highly expandable foam for lithographic 3D printing. *ACS applied materials & interfaces* 12, 16 (2020), 19033–19043.

[66] Gaojian Wu, Pengcheng Xie, Huaguang Yang, Kaifang Dang, Yuxuan Xu, Mohini Sain, Lih-Sheng Turng, and Weimin Yang. 2021. A review of thermoplastic polymer foams for functional applications. *Journal of Materials Science* 56 (2021), 11579–11604.

[67] Jinyuan Yang, Soumyabrata Dev, and Abraham G Campbell. 2024. RenderKernel: High-level programming for real-time rendering systems. *Visual Informatics* 8, 3 (2024), 82–95.

[68] Yue Yang, Lei Ren, Chuang Chen, Bin Hu, Zhuoyi Zhang, Xinyan Li, Yanchen Shen, Kuangqi Zhu, Junzhe Ji, Yuyang Zhang, et al. 2024. SnapInflatables: Designing Inflatables with Snap-through Instability for Responsive Interaction. In *Proceedings of the 2024 CHI Conference on Human Factors in Computing Systems*. 1–15.

[69] Zekun Yang, Yunlong Zhao, Yihui Lan, Menghui Xiang, Guirong Wu, Junbin Zang, Zhidong Zhang, Chenyang Xue, and Libo Gao. 2024. Screen-printable iontronic pressure sensor with thermal expansion microspheres for pulse monitoring. *ACS Applied Materials & Interfaces* 16, 30 (2024), 39561–39571.

[70] Jiakun Yu, Supun Kuruppu, Biyon Fernando, Praneeth Bimsara Perera, Yuta Sugiura, Sriram Subramanian, and Anusha Withana. 2024. IrOnTex: Using Ironable 3D Printed Objects to Fabricate and Prototype Customizable Interactive Textiles. *Proceedings of the ACM on Interactive, Mobile, Wearable and Ubiquitous Technologies* 8, 3 (2024), 1–26.

[71] Jiakun Yu, Praneeth Bimsara Perera, Rahal Viddusha Perera, Mohammad Mirkhalaf Valashani, and Anusha Withana. 2024. Fabricating customizable 3-D printed pressure sensors by tuning infill characteristics. *IEEE Sensors Journal* 24, 6 (2024), 7604–7613.